jove

Corneal and Limbal Alkali Injury Induction Using a Punch-Trephine Technique in a Mouse Model

Athar Shadmani[1], **Hala Shakib Dhowre**[1], **Ozlem Ercal**[1], **Xiang Qi Meng**[2], **Albert Y. Wu**[1]

[1] Department of Ophthalmology, Stanford University School of Medicine [2] McGill University Faculty of Medicine and Health Sciences

Corresponding Author

Albert Y. Wu
awu1@stanford.edu

Citation

Shadmani, A., Dhowre, H.S., Ercal, O., Meng, X.Q., Wu, A.Y. Corneal and Limbal Alkali Injury Induction Using a Punch-Trephine Technique in a Mouse Model. *J. Vis. Exp.* (198), e65609, doi:10.3791/65609 (2023).

Date Published

August 4, 2023

DOI

10.3791/65609

URL

jove.com/video/65609

Abstract

The cornea is critical for vision, and corneal healing after trauma is fundamental in maintaining its transparency and function. Through the study of corneal injury models, researchers aim to enhance their understanding of how the cornea heals and develop strategies to prevent and manage corneal opacities. Chemical injury is one of the most popular injury models that has extensively been studied on mice. Most previous investigators have used a flat paper soaked in sodium hydroxide to induce corneal injury. However, inducing corneal and limbal injury using flat filter paper is unreliable, since the mouse cornea is highly curved. Here, we present a new instrument, a modified biopsy punch, that enables the researchers to create a well-circumscribed, localized, and evenly distributed alkali injury to the murine cornea and limbus. This punch-trephine method enables researchers to induce an accurate and reproducible chemical burn to the entire murine cornea and limbus while leaving other structures, such as the eyelids, unaffected by the chemical. Moreover, this study introduces an enucleation technique that preserves the medial caruncle as a landmark for identifying the nasal side of the globe. The bulbar and palpebral conjunctiva, and lacrimal gland are also kept intact using this technique. Ophthalmologic examinations were performed via slit lamp biomicroscope and fluorescein staining on days 0, 1, 2, 6, 8, and 14 post-injury. Clinical, histological, and immunohistochemical findings confirmed limbal stem cell deficiency and ocular surface regeneration failure in all experimental mice. The presented alkali corneal injury model is ideal for studying limbal stem cell deficiency, corneal inflammation, and fibrosis. This method is also suitable for investigating pre-clinical and clinical efficacies of topical ophthalmologic medications on the murine corneal surface.

Introduction

The cornea is critical for vision and exhibits unique characteristics, including transparency, which is a prerequisite for clear vision. In addition to serving a major protective role, the cornea accounts for 2/3 of the refractive power of the eye[1]. Due to its significant role in vision, corneal injuries and opacity cause significant visual decline and are responsible for the second-highest cause of preventable blindness worldwide[2,3]. In corneal injuries with severe limbal dysfunction, the barrier function of the limbus decreases, resulting in the migration of conjunctival cells toward the corneal surface and corneal conjunctivalization[4,5], which compromises vision dramatically. Effective preventive and therapeutic strategies are therefore required to address the global burden of corneal blindness and related disability.

The current understanding of the human corneal wound healing process is based on previous studies that have investigated corneal responses to various injuries. Several techniques and animal models have been employed to induce various chemical or mechanical corneal injuries[6,7,8,9] and to investigate various aspects of the corneal wound healing process.

The alkali burn model is a well-established injury model which is performed by applying sodium hydroxide (NaOH) over the corneal surface directly or by using flat filter paper[10]. An alkali injury results in the release of pro-inflammatory mediators and infiltration of polymorphonuclear cells not only in the cornea and anterior chamber of the eye but also in the retina. This induces unintended retinal ganglion cell apoptosis and $CD45^+$ cell activation[11]. Therefore, it is critical to localize the injury site precisely to avoid excessive unintended injury using an alkali injury model.

The axial length of the murine eyeball is approximately 3 mm[12]. Due to this short distance between the cornea and the retina, a steep corneal curvature exists to provide high refractive power to focus the light on the retina (**Figure 1A**). As we previously reported[13], inducing chemical injury to this highly-curved surface using a flat filter paper is difficult, particularly at the limbus (**Figure 1B**). Inducing injury to the limbus requires tilting the filter paper, which has the potential to cause unintended injury to the fornix and adjacent conjunctiva[14]. Another approach involves directly applying the chemical agent as drops onto the corneal surface. However, this method lacks control over the exposure time, and there is a potential risk of inducing injury to the conjunctiva, fornix, and eyelids due to the diffusion of the liquid to these areas.

To overcome these limitations, this study presents a novel punch-trephine method to induce injury. This technique has several advantages including (i) inducing an effective chemical injury to the entire corneal surface and limbus in mouse model, (ii) inducing a localized and well-circumscribed injury to the cornea, (iii) the ability to apply any liquid of interest for a predetermined duration, and (iv) the ability to induce different sizes of corneal injuries by selecting appropriate biopsy punches. This method is also feasible for rat and rabbit injury models, which also exhibit a curved corneal surface and are common animal models used to study ocular surface wound healing.

Protocol

All procedures were carried out in accordance with the Stanford laboratory animal care APLAC number 33420, use of animals for scientific purposes, and the ARVO Statement

for the use of animals in ophthalmic and vision research. A total of 10 male and female C57BL/6 mice aged 8-12 weeks were generously provided by the Irving L. Weissman laboratory. The animals were acclimatized to a 12 h light-dark cycle and provided with water and feed *ad libitum*. Injury was induced to one eye of the animal.

1. Preparation for the experiment

1. Preparation of materials

   NOTE: All reagents are to be maintained at room temperature.

   1. Prepare the punch-trephine: Prepare a biopsy punch with a diameter of 3.5 mm and mark the shaft of the punch 5 mm away from its distal edge. Affix the punch firmly and cut the marked distal part of its shaft using a two-speed rotary tool. Wear ocular protection during this process. Cut the shaft at 3.5 mm depth and leave the final 1.5 mm attached. Bend the tip 90˚, as shown in **Figure 1**.
   2. Prepare 0.5 M NaOH solution by dissolving 1 g NaOH in 50 mL of distilled water.
   3. Prepare 10 mL of anesthetic cocktail by combining 2 mL of 100 mg/mL ketamine and 1 mL of 20 mg/mL xylazine. Prior to injection, dilute this mixture with 7 mL of 0.9% NaCl (normal saline).
   4. Prepare 0.1% fluorescein sodium solution by adding 0.1 mL of 10% AK-Fluor fluorescent liquid into 9.9 mL of sterile phosphate-buffered saline (1x PBS).
   5. Prepare PBS (1x) by dissolving 8 g NaCl, 0.2 g KCl, 1.44 g Na_2HPO_4, and 0.23 g NaH_2PO_4in 900 mL of distilled water. Adjust the pH of the solution to 7.4. Bring the solution to a final volume of 1 L by adding distilled water.
   6. Prepare 4% paraformaldehyde (PFA) solution for fixation. Under a chemical hood, dissolve 2 g PFA in 45 mL of PBS. Heat the mixture to 65 °C and titrate its pH to 7.4. Once the PFA has dissolved, bring the solution to a final volume of 50 mL.

2. Animal preparation

1. Weigh the mouse to determine the appropriate volume of injectable anesthetic cocktail for injection. After properly handling and restraining the mouse as described in Machholz et al.[15], administer the anesthetic cocktail intraperitoneally (IP) at a dose of 0.01 mL/g[16,17]. Target the inferior abdominal quadrants for IP injection to prevent organ damage.
2. Inject buprenorphine extended-release injectable suspension (3.25 mg/kg) subcutaneously for additional analgesia during and after surgery as corneal alkali injury is extremely painful.
3. Wait until a deep plane of anesthesia is achieved. Check for a lack of response to toe pinch as an indication of a successful deep plane of anesthesia. Apply simple eye ointment for the contralateral eye to prevent it from dryness before starting surgery.
4. After anesthesia, place the mouse on the surgical table prepared according to standard rodent surgery principles[18]. Place a 5 mm high pillow under the rodent's head, positioned in the lateral decubitus position. The pillow helps support the rodent's head during surgery.
5. Administer tetracaine hydrochloride (0.5%) eye drops for further anesthesia. Properly dry the ocular surface with a surgical eye spear and trim the eyelashes.

3. Induction of alkali injury

1. Before starting surgery, organize the surgery table as per standard rodent surgery principles[18,19] and keep the surgical field sterile during surgery. Position the surgical microscope to properly visualize the anesthetized mouse and adjust the timer to 30 s. Place a twisted paper towel onto the animal's muzzle to prevent unintended nasal aspiration during the rinsing process.
2. Determine the limbal area circumference using the surgical microscope while ensuring that the eyelids of the mouse are wide open using the thumb and index fingers. Gently hold the clean punch-trephine parallel to the axis of the eye, without applying any downward pressure. Avoid twirling the instrument and keep the axis of the punch-trephine parallel to the axis of the globe.
3. Ask the surgical assistant to drop 3 drops of NaOH solution (equal to 40 µL) into the punch-trephine's hole to fill the tool and cover the corneal surface appropriately. The surface tension of the liquid prevents any leakage out of the instrument (**Figure 1**).
   NOTE: We utilized a 1 mm syringe with a 27G needle featuring a flattened tip angled at 50° to carefully drop the NaOH solution.
4. After 30 s, immediately rinse the cornea and fornix with 5 mL of PBS (1x). **Video 1** demonstrates the procedure for inducing chemical injury.
5. Use a universal pH indicator paper to ensure a pH of 7 - 7.5 on the corneal surface of the injured eye. Then, apply the triple-antibiotic ophthalmic ointment over the chemically injured ocular surface.
   NOTE: Tail movement during surgery is a sign of low anesthetic depth. Apply additional anesthetic cocktail (ketamine+ xylazine) by injecting an anesthetic [bolus IP (50% of the initial volume)].
6. After surgery, confirm that the mouse is in a stable condition. Administer second buprenorphine if the animal is in pain. Use the same handling technique as in 2.2. Start the postoperative examination while the animal is under anesthesia.
7. After the procedure, wash, dry and sanitize the punch-trephine and the surgical table with 70% ethanol.

4. Clinical evaluation

1. For examination, anesthetize the mouse as previously described in step 2.1.
2. Examine the eyes (injured and non-injured) under a slit-lamp biomicroscope. Use a camera to capture photos (in this study, a phone camera in Cinematic mode was used).
3. Score corneal opacity according to the Yoeruek grading system[20]: 0 = normal, clear cornea; 1 = mild opacity; 2 = greater opacity, but the iris and pupil are easily distinguishable; 3 = iris and pupil are barely distinguishable; 4 = cornea is completely opaque with an invisible pupil.
4. Apply 0.1% fluoresceine eye drops. Dry excess fluorescent liquid with a cotton applicator and evaluate for the presence of corneal epithelial defects using the cobalt blue filter. Capture photos.
5. Monitor the animal until it regains sufficient consciousness to maintain sternal recumbency. Do not reintroduce the animal to other animals until it has completely recovered.

5. Enucleation

1. Euthanize mice 2 weeks after chemical injury induction by cervical dislocation in 3-5 s[21].
2. Enucleate the eye while preserving the medial caruncle and whole palpebral conjunctiva in the following order, as shown in **Video 2**.
3. Under the surgical microscope, carefully dissect the junction of the caruncle and skin. Using tooth forceps, retract the caruncle and guide the tip of surgical scissors under the palpebral conjunctiva towards its junction with the tarsal plate.
4. Cut the conjunctiva along the adhesion line towards the lateral canthus. Then, turn the surgical scissors to the junction of the conjunctiva and inferior tarsal plate at the subconjunctival plane.
5. After completing conjunctival dissection, retract the superior and inferior eyelids from the nasal side with the thumb and index fingers. While retracting, guide the tip of a curved-tip tweezer behind the protruded lacrimal glad towards the optic nerve. Firmly grasp the optic nerve and extract the globe (**Figure 2**).
6. Rinse the globe with PBS (1x) and transfer it into the fixating solution.

6. Hematoxylin and eosin (H&E) and periodic acid-Schiff (PAS) staining

1. Fix the globes in 10% formalin solution overnight at room temperature.
2. Dehydrate the tissues using a sequential series of graded alcohol with concentrations of 70% ethanol, 80% ethanol, 90% ethanol, and 100% ethanol, each for 10-15 min. Subsequently, immerse the eyes in xylene for 10 min. Finally, encase the eyes in paraffin.
3. Section the paraffin blocks into 6 µm thick slices and mount them on glass microscope slides for hematoxylin and eosin (H&E) and periodic acid-Schiff (PAS) staining, as described in **Supplementary File 1**.

7. Immunofluorescence imaging and analysis

1. For immunohistochemistry studies (IHC), fix the eyes in 1 mL of PBS (1x) containing 4% PFA at 4 ˚C overnight. Wash the sample 3x in 1 mL of PBS (1x) for 5 min each.
2. To prevent ice crystal formation and to protect the molecular structures of the proteins, perform serial sucrose saturation with 10% sucrose, 20% sucrose, and 30% sucrose concentrations in PBS. Embed the globes in optical coherence tomography solution (OCT; **Figure 2**), and store them at -80 °C.
3. Section the OCT block into 12 µm thick slices and mount on glass microscope slides for IHC staining.
4. Permeabilize tissue sections on microscope slides in 0.1% Triton X −100 in PBS (1x) for 15 min. Then, block nonspecific antigens with 5% BSA in PBS (1x) for an additional 1 h at room temperature.
5. Incubate tissue sections on microscope slides at 4 °C overnight in the cocktail of the targeted primary antibodies prepared in PBS (1x) containing 1% BSA. In this experiment, the primary antibodies were 1:100 diluted rabbit anti-keratin 13 (K13) and anti-keratin 12 (K12) antibodies with concentration of 2.24 µg/mL and 1.56 µg/mL, respectively.
6. After incubation, wash the tissue sections on microscope slides 3x with PBS (1x). Subsequently, detect bound primary antibodies with 1:500 diluted donkey anti-rabbit-

IgG. Incubate with the secondary antibody at 4 ˚C for 1 h in the dark. Then wash in PBS (1x) 3x for 5 min each.

7. Apply a drop of anti-fade fluorescence mounting medium containing DAPI on the tissue sections on microscope and cover with a coverslip. Allow samples to dry in the dark and examine them under a fluorescent microscope with the same laser setting for normal and injured eyes.

Representative Results

The efficacy of the method in inducing limbal stem cell deficiency (LSCD) was assessed by evaluating the clinical and histological signs of LSCD. Clinical assessment was done by slit-lamp microscopy and anterior segment- optical coherence tomography (AS-OCT) imaging (**Figure 3** and **Figure 4**).

Re-epithelialization occurred in a centripetal manner and was faster at the temporal part of the cornea compared to its nasal part. Injured eyes developed 2^+-3^+ corneal haze immediately after chemical injury (**Figure 3**). Epithelial cells migrated from the conjunctiva to the corneal surface following limbal injury. The large corneal epithelial defect was re-epithelialized completely on days 12-14, which took longer compared to a corneal epithelial injuryof similar size and intact basement membrane and stroma which typically healed within 5 days post-injury[8,9]. Due to LSCD, 50% of the injured eyes developed persistent epithelial defects at the end of second week (**Figure 3**). Corneal edema was more prominent during the first few days (**Figure 3**, **Figure 4**), whereas corneal fibrosis was significant in the second week that resulted in 4^+ corneal opacity in 100% of injured eyes.

Early signs of neovascularization (NV) were observed clinically and histologically, 24 h after chemical injury induction, as illustrated in **Figure 5**, consistent with the timeline of NV identified by Kvanta et al. study that showed sign of limbal NV 24 h after injury[22]. During the healing process, new vessels matured and by the 14th day after injury, NV crossed the limbus and reached the central cornea. The limbus, which defines the boundary between the conjunctiva and cornea, was destroyed.

Histological evidence of limbal stem cell deficiency and conjunctivalization were observed by the appearance of PAS + goblet cells and stromal blood vessels[23,24,25,26]. Goblet cells were observed in the present injury model and indicated by the arrow in **Figure 6.**

Conjunctival and corneal epithelia principally express unique keratins, K13 and K12, respectively[27]. After the limbal injury, new epithelial cells that originated from the conjunctiva covered the denuded cornea, and K12 was not expressed on the corneal surface of any injured animals during 2 weeks after injury. This finding, consistent with other studies[28], indicated complete LSCD and the absence of corneal epithelial cells on the corneal surface. However, in the study by Park et al.[29], they detected K12 expression 20 and 32 weeks after injury, suggesting a possible trans-differentiation of the epithelial cells.

Consequently, we observed that chemical injury destroyed the limbus and limbal stem cells which resulted in the migration of conjunctival epithelial cells to the center of the cornea to cover the denuded corneal surface. This is further validated by the conjunctival epithelial cell marker, K13, which was expressed in the entire conjunctiva and corneal surfaces as shown in **Figure 7**.

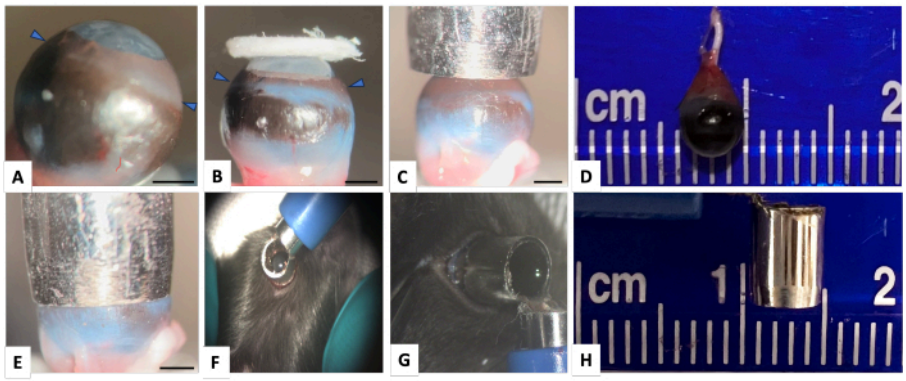

Figure 1: Normal mouse right eye and the punch-trephine for inducing corneal and limbal injury. (**A**) Lateral view showing mouse eye with highly curved cornea (arrowheads indicate the limbus). (**B**) The image demonstrates that even a large filter paper is insufficient to adequately cover the limbal area. The limbus-to-limbus diameter of the mouse eye is almost 4 mm and a punch biopsy with an external diameter of 4.5 mm and internal diameter of 3.5 mm (panels **D** and **H**), appropriately covers the cornea and limbal surface as shown in panels (**C**) and (**E**). (**F**) The punch-trephine is appropriately held over the globe around the limbal area. (**G**) To ensure that there is no leakage through the edge of the punch-trephine, after appropriately positioning the punch-trephine in a parallel axis with the globe, the hole is filled with methylene blue. No leakage of methylene blue is detected. Scale bar = 1 mm. Please click here to view a larger version of this figure.

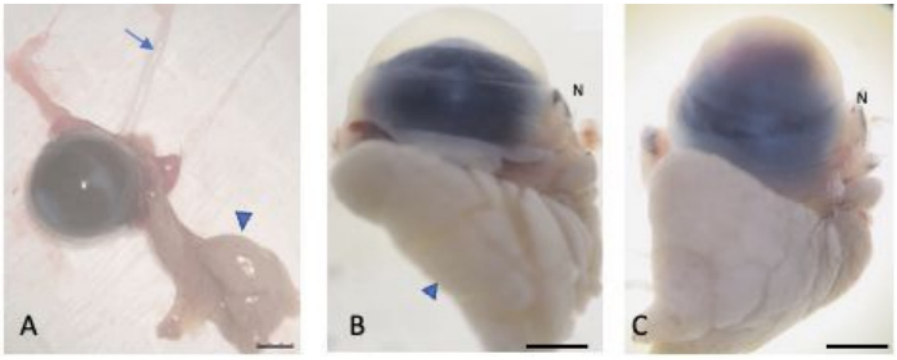

Figure 2: Enucleated eyes. (**A**) The eyes were enucleated while preserving the bulbar and palpebral conjunctiva, the lacrimal gland (arrowhead), and the optic nerve (arrow). The normal (**B**) and injured (**C**) eyes were saturated in 30% sucrose to protect against cryocrystal formation. The nasal part of the globe is recognizable through the nasal caruncle (labelled N). Scale bar = 1 mm. Please click here to view a larger version of this figure.

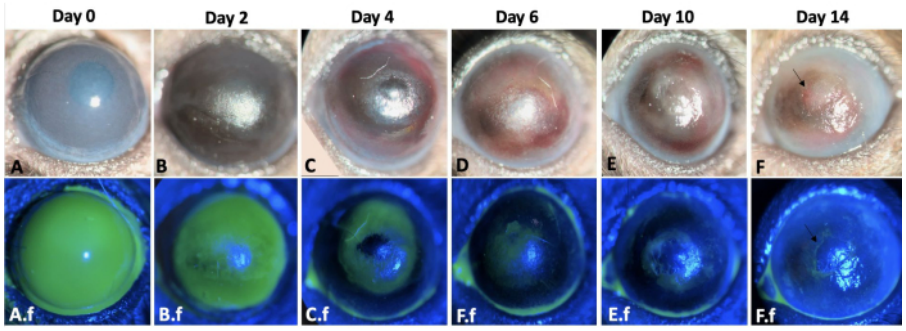

Figure 3: Wound healing of the left eye. The wound healing process of the left mouse eye throughout 2 weeks after corneal and limbal alkali injury in a mouse model is shown here (**A-F**). The slit lamp examination of the eye. Corneal edema is more prominent on days 0 and 2 (A,B), whereas fibrosis is more evident during the second-week post-injury (E-F). **A.f-F.f** show the re-epithelialization process of the same eye. Total corneal and limbal epithelial defect immediately after injury induction is observed in A.f. The epithelial defect healed by conjunctival epithelial cell migration in a centripetal pattern by 12-14 days (A.f-F.f). However, 50% of the injured eyes developed persistent epithelial defect at the end of second week as shown by arrow in F and F.f images. Scale bar = 1 mm (panel C). Please click here to view a larger version of this figure.

Figure 4: Anterior segment OCT of the mouse eye. (**A**) AS-OCT illustrates normal cornea curvature and anterior chamber. The iris structure is well-defined and recognizable. No iridocorneal adhesion is detectable at the mid-periphery of the iris. (**B**) Immediately after injury the corneal thickness increases due to edema formation and iridocorneal adhesion develops at the mid periphery of the iris. (**C**) Two weeks after injury the corneal curvature has changed and total iridocorneal adhesion with anterior chamber destruction is visible. Scale bar = 1 mm. Please click here to view a larger version of this figure.

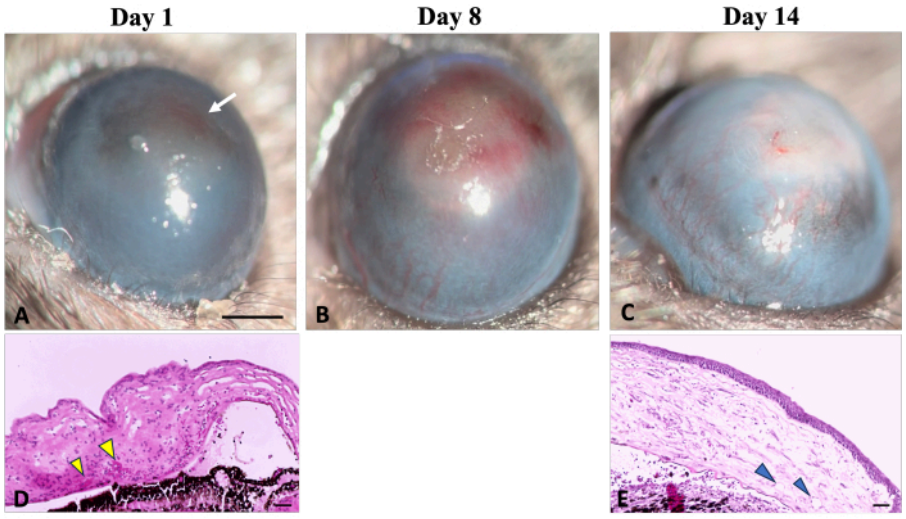

Figure 5: Corneal neovascularization. Clinical and histological signs of corneal neovascularization can be observed during the wound healing process following sodium hydroxide (NaOH) injury. (**A**) The initial signs of neovascularization become detectable on the first day after injury, characterized by a reddish discoloration of the cornea (indicated by a white arrow). This discoloration results from the aggregation of red blood cells in the stroma, as illustrated in corresponding histological image (**D**) (indicated by yellow arrowheads). (**B**) Over the first week of regeneration, new vessels progressively increase and spread throughout the cornea. (**C**) By the end of 2 weeks, the limbal area is destroyed, and the new vessels continue to evolve. (**E**) The histological section of the cornea further illustrates the presence of deep stromal neovascularization (shown by arrowheads). Slit lamp Image scale bar = 1 mm, the histology image scale bar = 50 µm. Please click here to view a larger version of this figure.

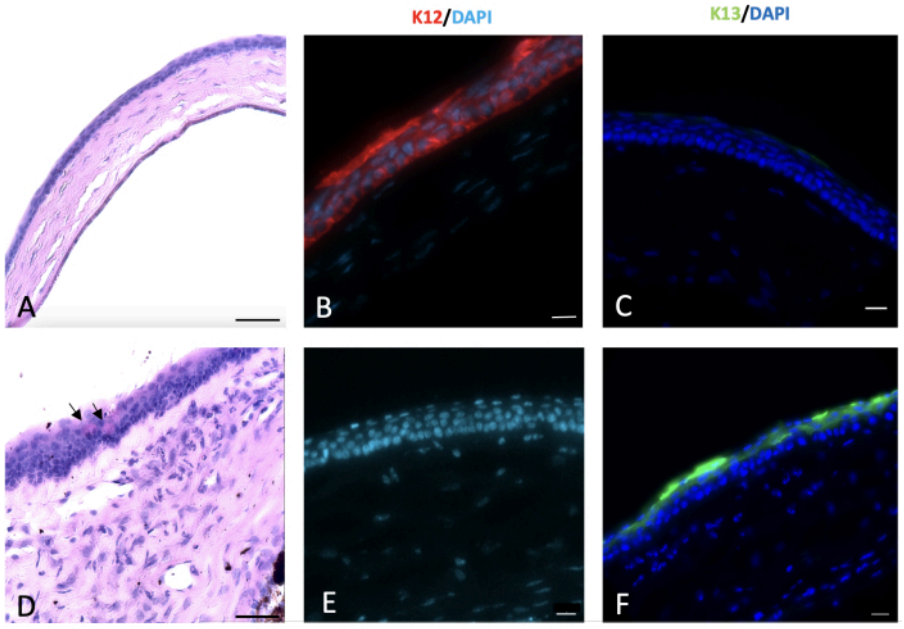

Figure 6: Periodic acid-Schiff and immunohistochemical (IHC) staining of cornea. Periodic acid-Schiff and immunohistochemical staining of the normal and injured cornea was done 2 weeks post-injury. Normal mouse corneal epithelium composed of 4-5 layers of cells (**A**). Alkali injury to the cornea and limbus led to conjunctivalization of the cornea with appearance of goblet cells on the corneal surface as shown by black arrows in (**D**). Normal corneal epithelial cells express K12 (**B**), which is not expressed by the conjunctival cells that cover the injured cornea (**E**). K13, a characteristic marker of conjunctival epithelial cells, is not expressed on the normal corneal epithelial cells (**C**). However, it is present on the sodium hydroxide (NaOH) injured corneal surface that is a sign of corneal conjunctivalization (**F**). Histology image scale bar = 50 µm, IHC stained image scale bar = 20 µm. Please click here to view a larger version of this figure.

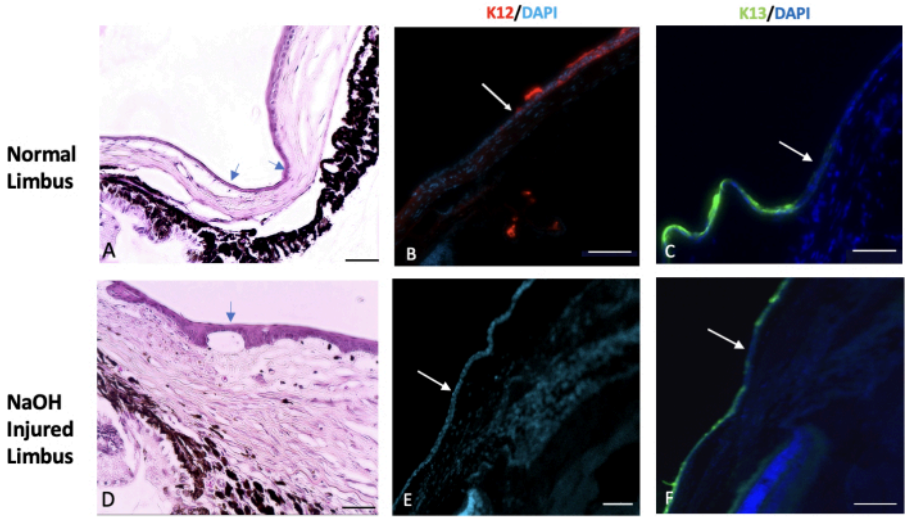

Figure 7: Hematoxylin and eosin and immunohistochemical staining. Hematoxylin and eosin (H&E) and immunohistochemical staining of the normal and injured limbus tissue was done. (**A**) The normal limbus marks the transition area between the end of the sclera and the beginning of the cornea. This region is typically covered by one or two layers of conjunctival epithelial cells (indicated by the arrows). In a healthy eye, the expression of a specific corneal epithelial marker called K12 begins at the limbus and extends to the surface of the cornea (shown in image **B**). On the other hand, the expression of a conjunctival marker known as K13 is restricted to the limbus and does not extend beyond it (indicated by the white arrow in image **C**). In eyes injured by sodium hydroxide (NaOH), the boundaries of the limbus are disrupted. This leads to migration of conjunctival cells towards the injured cornea. (**D**) The images of the NaOH-injured limbus demonstrate the presence of neovascularization both beneath the epithelial layer and within the stromal tissue. Following the injury, the injured corneal surface lacks the presence of K12 (**E**), while K13 is abundantly expressed on the corneal surface (**F**). Histology image scale bar = 50 µm, IHC stained image scale bar = 100 µm. Please click here to view a larger version of this figure.

Supplementary File 1: Staining protocol. Please click here to download this File.

Video 1: NaOH corneal and limbal injury in a mouse model with a punch-trephine. The video demonstrates the procedure of inducing NaOH corneal and limbal injury in a mouse model with a punch-trephine. It is crucial to hold the punch-trephine in a parallel axis with the globe and apply minimal pressure to the limbus. This proper technique is essential to prevent leakage and achieve optimal results. Please click here to download this Video.

Video 2: Illustration of the enucleation technique while preserving the bulbar conjunctiva. To differentiate the nasal side of the globe from the temporal side, the nasal caruncle is preserved along with the globe. The entire conjunctiva is dissected starting from its junction to the tarsal plate. With minimal pressure, the orbital contents protrude

outward. By guiding the forceps toward the back of the globe, the optic nerve is grasped, and the tissue is extracted. The enucleated tissue includes the globe, orbital fat, and orbital lacrimal gland. Please click here to download this Video.

Discussion

This study proposes an innovative device, the punch-trephine, which can be used to successfully induce an effective and reproducible corneal and limbal injury in a mouse model. This limbal stem cell deficiency model is ideal to investigate the dynamics of corneal wound healing and conjunctivalization after injury.

Evidence suggests that both the limbal niche and central part of the murine cornea contain stem cells[30]. Therefore, an efficient corneal and limbal injury is required to produce a stem cell deficiency model, and the injury model presented here enables exposure of the curved corneal limbus to a chemical agent for a specific period. To determine the best concentration and duration of NaOH injury, injuries were inflicted with various NaOH concentrations and durations. Higher NaOH concentrations or longer exposure durations resulted in increased tissue damage and fibrosis. Therefore, researchers can adjust these parameters based on the specific goals of their study and the desired severity of injury.

To successfully reproduce this corneal and limbal injury model, several key considerations should be considered. First, it is imperative to measure the limbal-to-limbal diameter of the targeted eye to determine the appropriate size of the punch. Selecting a biopsy punch with an external diameter that is 0.5 - 1 mm larger than this diameter is recommended.

The surface tension of the liquid used is an important factor in preventing leakage at the interface between the ocular surface and the edge of the punch trephine as shown in **Figure 1G**. Therefore, there is no need to apply pressure to the tip of the punch biopsy.

To avoid causing mechanical damage to the tissue, it is critical to hold the punch trephine in a parallel axis with the eye and refrain from applying pressure to the limbus. Improper adjustment of the punch trephine axis can increase the risk of leakage and result in a decentered site of injury and inaccurate results.

Some potential limitations of this technique include the need to select the appropriate punch size, acquiring proficiency in holding the punch trephine, and the potential risk of causing mechanical injury. However, these limitations can be overcome through practice and by following the instructions outlined in this protocol. The strain and the age range of the mice are other factors that affect the re-epithelialization process and must be considered in the study.

Moreover, the proposed protocol is advantageous as it details an enucleation method that preserves the bulbar and palpebral conjunctiva and allows for the determination of the nasal part of the globe without the application of surgical sutures as a marker. Previous research has indicated that the nasal region of the eye possesses the lowest neural innervation compared to other areas of the cornea, which makes it more vulnerable to neovascularization and reduced regenerative efficacy[31,32].

In summary, the clinical signs of LSCD, such as corneal opacity (CO), persistent epithelial defects, and corneal neovascularization (NV), along with the observed histological changes, including goblet cell metaplasia, expression of K13 on the corneal surface, and absence of K12 on the corneal surface, confirm the presence of LSCD in this model. These findings provide evidence that this novel technique

is effective in inducing LSCD. This chemical injury model can be employed in preclinical studies to investigate new medications and pharmaceutical treatments in the field of corneal injury and regeneration.

Disclosures

None of the authors have any financial interest in any of the companies or products described in this study. The authors declare no other conflicts of interest.

Acknowledgments

We acknowledge that NEI P30-EY026877 supports this research. We greatly acknowledge Charlene Wang and the Dr. Irv Weissman Lab at Stanford University's Institute for Stem Cell Biology and Regenerative Medicine for all their kind assistance in providing experimental animals. We appreciate Hirad Rezaeipoor's assistance in the preparation and editing of the images.

References

1. Sridhar, M. S. Anatomy of cornea and ocular surface. *Indian Journal of Ophthalmology.* **66** (2), 190-194 (2018).
2. Robaei, D., Watson, S. Corneal blindness: a global problem. *Clinical & experimental Ophthalmology.* **42** (3), 213-214 (2014).
3. Lamm, V., Hara, H., Mammen, A., Dhaliwal, D., Cooper, D. K. C. Corneal blindness and xenotransplantation. *Xenotransplantation.* **21** (2), 99-114 (2014).
4. Danjo, S., Friend, J., Thoft, R. A. Conjunctival epithelium in healing of corneal epithelial wounds. *Investigative Ophthalmology & Visual Science.* **28** (9), 1445-1449 (1987).
5. Shapiro, M. S., Friend, J., Thoft, R. A. Corneal re-epithelialization from the conjunctiva. *Investigative Ophthalmology & Visual Science.* **21** (1 Pt 1), 135-142 (1981).
6. Shah, D., Aakalu, V. K. Murine Corneal Epithelial Wound Modeling. in *Wound Regeneration: Methods and Protocols.* (ed. Das, H.) 175-181. Springer US (2021).
7. Rittié, L., Hutcheon, A. E., Zieske, J. D. Mouse models of corneal scarring. *Fibrosis: Methods and Protocols.* **1627**, 117-122 (2017).
8. Stepp, M. A. et al. Wounding the cornea to learn how it heals. *Experimental Eye Research.* **121**, 178-193 (2014).
9. Akowuah, P. K., De La Cruz, A., Smith, C. W., Rumbaut, R. E., Burns, A. R. An Epithelial Abrasion Model for Studying Corneal Wound Healing. *Journal of Visualized Experiments.* (178), 63112 (2021).
10. Bai, J.Q., Qin, H.F., Zhao, S.H. Research on mouse model of grade II corneal alkali burn. *International journal of ophthalmology.* **9** (4), 487-490 (2016).
11. Paschalis, E. I. et al. The Role of Microglia and Peripheral Monocytes in Retinal Damage after Corneal Chemical Injury. *The American Journal of Pathology.* **188** (7), 1580-1596 (2018).
12. Jiang, M. et al. Single-Shot Dimension Measurements of the Mouse Eye Using SD-OCT. *Ophthalmic Surgery, Lasers and Imaging Retina.* **43** (3), 252-256 (2012).
13. Shadmani, A., Razmkhah, M., Jalalpoor, M. H., Lari, S. Y., Eghtedari, M. Autologous Activated Omental versus Allogeneic Adipose Tissue-Derived Mesenchymal Stem Cells in Corneal Alkaline Injury: An Experimental Study. *Journal of Current Ophthalmology,. 33* (2), 136-142 (2021).

14. Swarup, A. et al. PNP Hydrogel Prevents Formation of Symblephara in Mice After Ocular Alkali Injury. *Translational Vision Science & Technology.* **11** (2), 31-31 (2022).
15. Machholz, E., Mulder, G., Ruiz, C., Corning, B. F., Pritchett-Corning, K. R. Manual restraint and common compound administration routes in mice and rats. *Journal of Visualized Experiments.* (67), 2771 (2012).
16. Jaber, S. M. et al. Dose Regimens, Variability, and Complications Associated with Using Repeat-Bolus Dosing to Extend a Surgical Plane of Anesthesia in Laboratory Mice. *Journal of the American Association for Laboratory Animal Science.* **53** (6), 684-691 (2014).
17. Navarro, K. L. et al. Mouse Anesthesia: The Art and Science. *ILAR Journal.* **62** (1-2), 238-273 (2021).
18. Hoogstraten-Miller, S. L., Brown, P. A. Techniques in Aseptic Rodent Surgery. *Current Protocols in Immunology.* **1**, 1.12.1-1.12.14 (2008).
19. ACLAM Medical Records Committee, et al. Medical Records for Animals Used in Research, Teaching, and Testing: Public Statement from the American College of Laboratory Animal Medicine. *ILAR Journal.* **48** (1), 37-41 (2007).
20. Yoeruek, E. et al. Safety, penetration and efficacy of topically applied bevacizumab: evaluation of eyedrops in corneal neovascularization after chemical burn. *Acta Ophthalmologica.* **86** (3), 322-328 (2008).
21. Shomer, N. H. et al. Review of rodent euthanasia methods. *Journal of the American Association for Laboratory Animal Science.* **59** (3), 242-253 (2020).
22. Kvanta, A., Sarman, S., Fagerholm, P., Seregard, S., Steen, B. Expression of Matrix Metalloproteinase-2 (MMP-2) and Vascular Endothelial Growth Factor (VEGF) in Inflammation-associated Corneal Neovascularization. *Experimental Eye Research.* **70** (4), 419-428 (2000).
23. Tseng, S. C., Hirst, L. W., Farazdaghi, M., Green, W. R. Goblet cell density and vascularization during conjunctival transdifferentiation. *Investigative Ophthalmology & Visual Science.* **25** (10), 1168-1176 (1984).
24. Huang, A. J., Tseng, S. C. Corneal epithelial wound healing in the absence of limbal epithelium. *Investigative ophthalmology & visual science.* **32** (1), 96-105 (1991).
25. Rama, P. et al. Limbal stem-cell therapy and long-term corneal regeneration. *New England Journal of Medicine.* **363** (2), 147-155 (2010).
26. Deng, S. X. et al. Global consensus on the definition, classification, diagnosis and staging of limbal stem cell deficiency. *Cornea.* **38** (3), 364-375 (2019).
27. Wei, Z. G., Wu, R. L., Lavker, R. M., Sun, T. T. In vitro growth and differentiation of rabbit bulbar, fornix, and palpebral conjunctival epithelia: Implications on conjunctival epithelial transdifferentiation and stem cells. *Investigative Ophthalmology and Visual Science.* **34** (5), 1814-1828 (1993).
28. Kao, W. W.Y. Keratin expression by corneal and limbal stem cells during development. *Experimental Eye Research.* **200**, 108206 (2020).
29. Park, M. et al. Plasticity of ocular surface epithelia: Using a murine model of limbal stem cell deficiency to delineate metaplasia and transdifferentiation. *Stem Cell Reports.* **17** (11), 2451-2466 (2022).

30. Li, J. et al. Identification for Differential Localization of Putative Corneal Epithelial Stem Cells in Mouse and Human. *Scientific Reports.* **7** (1), 5169 (2017).

31. McKenna, C. C., Lwigale, P. Y. Innervation of the Mouse Cornea during Development. *Investigative Ophthalmology & Visual Science.* **52** (1), 30-35 (2011).

32. He, J., Bazan, H. E. P. Neuroanatomy and Neurochemistry of Mouse Cornea. *Investigative Ophthalmology & Visual Science.* **57** (2), 664-674 (2016).